GlueX-doc-843
CVS: docs/bshield
Original: July 17, 2007
Updated: August 24, 2007

Calculations of magnetic shield effectiveness for long μ-metal cylinders

E.S. Smith

1 Overview

There are several Hall D systems that require photomultipliers which will be operated at various locations in the fringe field of the solenoid. Both the pulse height and timing resolution suffers when photomultiplier tubes are operated in magnetic fields as low as a few tenths of Gauss. Therefore most photomultiplier tubes will require some amount of passive magnetic shielding in our detector. Ultimately the configuration of the shield must be optimized for the specific operating conditions and particular orientation of the phototube in the magnetic field. However, analytical estimates of the shield effectiveness are very useful during the design stage in order to select alternatives for more detailed study. In this paper we work out the details of some specific examples for the case of a long cylindrical shield which is placed in a uniform magnetic field perpendicular to the tube axis, and compare them with some existing measurements.

2 Formalism

The magnetic shield effectiveness of an infinitely long cylinder with magnetic permeability μ, which is placed in a magnetic field perpendicular to the axis of the tube, is a solved magnetostatic problem and worked out in various E&M texts [1]. The tube has an inner radius a and outer radius b and is placed with its axis along the z-direction in a uniform magnetic field with an undisturbed magnet strength H_0 along the x-direction.

This problem is solved as a boundary-valued problem for the magnetic scalar potential V_m, where $\vec{H} = -\nabla V_m$. The three regions of the problem (1, 2 and 3) and the chosen coordinate system are shown in Fig. 1. The general solution is given by

$$V_1 = -H_0\, r \cos\theta + \frac{1}{r} B_1 \cos\theta \tag{1}$$

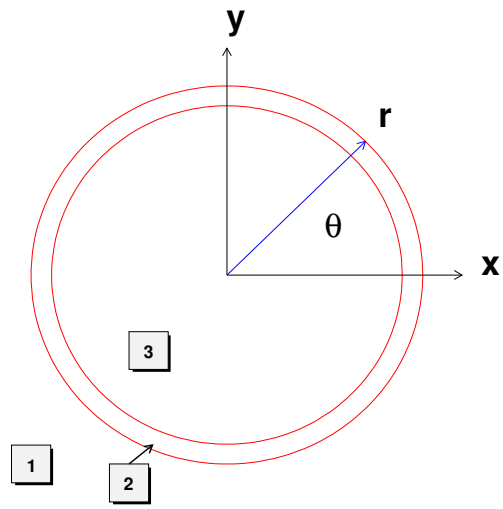

Figure 1: Geometry and coordinate system for calculation. The axis of the magnetic shield is oriented along the z-axis.The three regions are indicated by the boxes: region 1 outside the shield, region 2 in the μ-metal material itself, and region 3 constituting the area inside the shield.

$$V_2 = A_2\, r\cos\theta + \frac{1}{r} B_2 \cos\theta \tag{2}$$

$$V_3 = A_3\, r\cos\theta \tag{3}$$

Using the continuity conditions of the normal component of magnetic field B and the parallel component of the magnetic field strength H at both boundaries of the magnetic shield, the following conditions are obtained:

$$A_3 = -4\mu H_0 b^2/\Delta, \quad \Delta = b^2(1+\mu)^2 - a^2(1-\mu)^2 \tag{4}$$

$$-H_0\, b^2 + B_1 = A_2\, b^2 + B_2 \tag{5}$$

$$A_2\, a^2 + B_2 = -\mu\,(-A_2\, a^2 + B_2) \tag{6}$$

$$-H_0\, b^2 - B_1 = \mu\,(A_2\, b^2 - B_2), \tag{7}$$

where the first equation is solved explicitly in the references. In order to extract the other constants, the simultaneous equations can be solved with the following solution:

$$B_1 = H_0 b^2(\mu^2-1)(b^2-a^2)/\Delta \tag{8}$$

$$B_2 = -2H_0 b^2 a^2(\mu-1)/\Delta \tag{9}$$

$$A_2 = -2H_0 b^2(\mu+1)/\Delta \tag{10}$$

The solutions for the magnetic field strength in the three regions are obtained by differentiating V_m:

$$H_1 = H_0\,\hat{\imath} + \frac{1}{r^2}B_1\left(\cos 2\theta\,\hat{\imath} + \sin 2\theta\,\hat{\jmath}\right) \tag{11}$$

$$H_2 = -A_2\,\hat{\imath} + \frac{1}{r^2}B_2\left(\cos 2\theta\,\hat{\imath} + \sin 2\theta\,\hat{\jmath}\right) \tag{12}$$

$$H_3 = -A_3\,\hat{\imath} \tag{13}$$

It is interesting to note that the magnetic field strength inside the shield only has an x-component, i.e. is in the same direction as the unperturbed field, but reduced in intensity by a factor g called the shield effectiveness. The shield effectiveness can be computed readily as

$$g = \frac{H_0}{H_3} = \frac{b^2(1+\mu)^2 - a^2(1-\mu)^2}{4\mu b^2} \tag{14}$$

This reduces to the common expression for g in the limit of large μ of

$$g = \left(\frac{\mu}{4}\right)\left(\frac{b^2-a^2}{b^2}\right) \simeq \frac{\mu}{2}\left(\frac{t}{b}\right), \tag{15}$$

where we have introduced the thickness $t = (b-a)$ of the shield.

3 Applications

In order to apply the results from the previous section, we need the magnetic permeability of specific materials. Typical properties of μ-metal which is used in the fabrication of magnetic shields for photomultiplier tubes are given in Table 1 [2]. The

Table 1: Magnetic properties of Ad-Vance Magnetics magnetic alloys from http://www.advancemag.com/Materials.htm.

Magnetic Property	AD-MU-80	AD-MU-78	AD-MU-48	AD-MU-00
Initial Permeability at 40 G	75,000	60,000	11,500	300
Permeability at 100-200 G	100,000	43,000	20,000	13,000
Max. permeability	300,000	250,000	130,000	3,000
Saturation Induction (G)	8,000	7,600	15,500	22,000
Coercive Force (Oe)	0.015	0.010	0.050	1.000

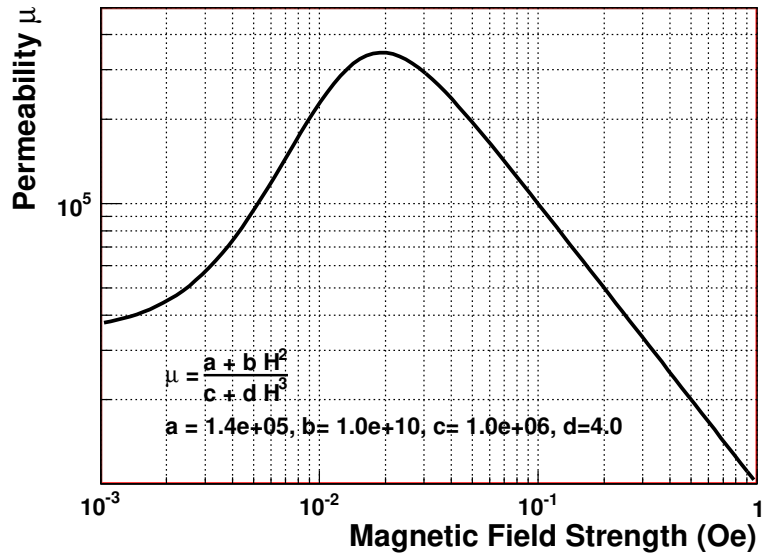

Figure 2: Parameterization of the permeability of typical high permeability material, such as AD-MU-78, as a function of the magnetic field strength.

permeability is a strong function of the magnetic field in the material and its typical behavior is shown in Fig. 2 as a function of the magnetic field strength H [3]. Note that the shielding problem has been solved assuming the material is not saturated with a constant value for the permeability μ. For the purpose of this study we make the assumption that the minimum value of the permeability within the shield will determine the effectiveness of the shield. This is because the magnetic flux lines must be continuous and any limitation in the strength of the field at some point in the material will reduce the intensity in the rest of the volume. The minimum value of μ is typically close to the quoted value at 40 G (H$\sim 10^{-3}$ Oe), unless the field strength exceeds about 0.2 Oe, which is well into saturation. The topic of saturation is explored in the next section.

4 Saturation

The qualitative behavior of the magnetic shield changes dramatically when the magnetic material begins to saturate. In this point, the cylinder stops behaving as a shield and allows the magnetic flux lines to pass unimpeded. The point of saturation can be estimated form Eq. 12. The magnetic flux density in the μ-metal shield can

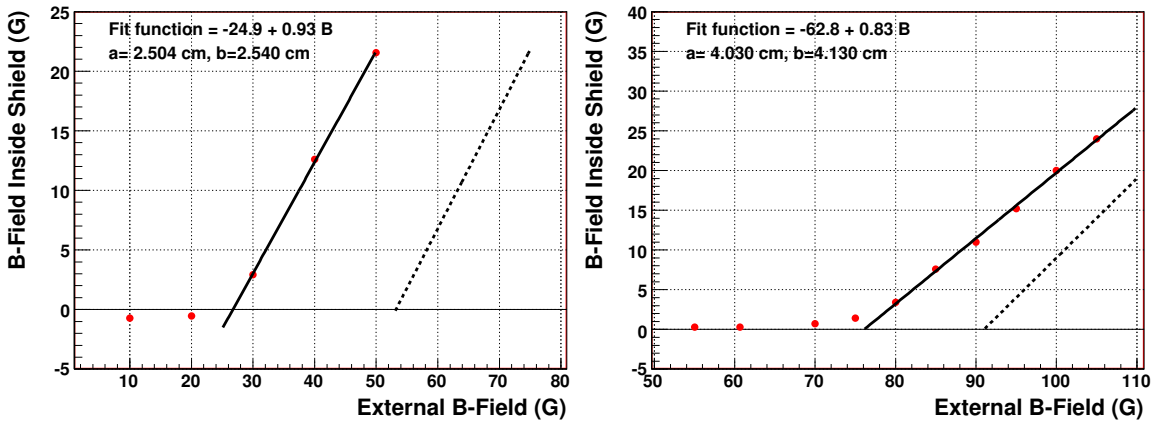

Figure 3: Measurements of the field inside two cylindrical shields as a function of the external magnetic flux for two difference cylinders and experimental configurations. In both cases the magnetic field was oriented perpendicular to the axis of the cylinder. The solid line is a fit to the data beyond saturation and the dashed line is the prediction assuming that the magnetic flux is effectively unshielded past the saturation point predicted by Eq. 18.

be calculated and reduces for $\mu \gg 1$ to the follwing expression:

$$\vec{B}_\mu = 2H_0 \left(\frac{b^2}{b^2 - a^2}\right) \left((1 - \cos 2\theta)\hat{\imath} - \sin 2\theta \hat{\jmath}\right) \tag{16}$$

$$B_\mu = 4H_0 \left(\frac{b^2}{b^2 - a^2}\right) |\sin\theta|, \tag{17}$$

where we are using this notation of B_μ for the magnetic field flux in the magnetic material (region 2) to avoid confusion with the coefficient in Eq. 9. We note that the flux density is independent of the magnetic permeability μ and depends only a geometric factor (area ratio of the outer circle to the area of the magnetic material) and the external field H_0. The magnetic flux at which the material saturates is a property of the magnetic material and is given in Table 1 for common magnetic shielding materials. For example AD-MU-78 saturates at $B_{sat} = 7600$ G. This expression allows us to compute the maximum external field which can be shielded effectively with a given material and cylindrical shape:

$$H_{max} = B_{sat} \left(\frac{b^2 - a^2}{4\,b^2}\right) \approx B_{sat} \left(\frac{t}{2\,b}\right), \tag{18}$$

where we have used the maxium value of field in the shield as a measure of when saturation ensues. The magnetic material will begin staturating at 90° and imme-

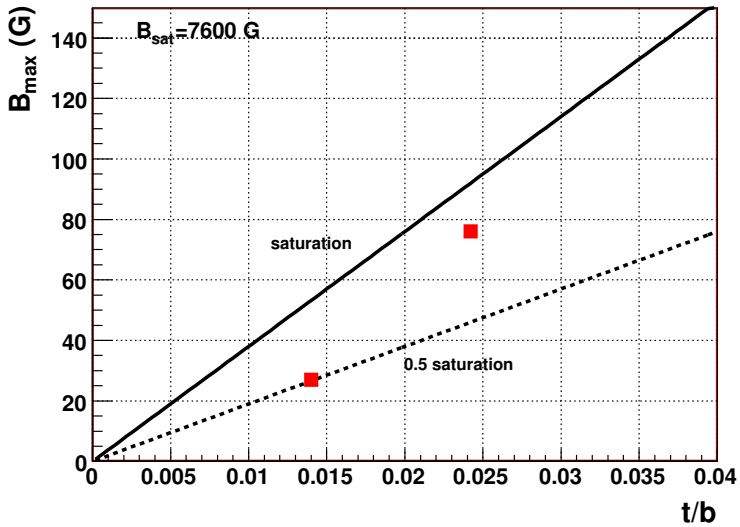

Figure 4: Maximum external magnetic field flux before the material begins to saturate as a function of the ratio of thickness to radius of the cylinder. The two measurements extracted from Fig. 3 indicate that the actual saturation field is only 0.5 and 0.8 of that specified by the manufacturer.

diately start effecting the effectiveness of the shield. The predicted saturation field given by Eq. 18 is compared with two sets of measurements [4, 5] which are shown in Fig. 3. The intercept extracted from the fit can be used to determine the external field where the material begins to saturate. This is plotted in Fig. 4 along with the expectation from Eq. 18. For materials in saturation, we assume that the field inside the cylinder is given by the difference between the external field and H_{max} given in Eq. 18. However this formula should be scaled down by a factor of 0.5 to 0.8 to match measured data from Fig. 3.

4.1 3" PMT Shields

We first compute the residual field in a 3.25" magnetic shield which can be compared to existing measurements [4, 6]. The shield was a 32P80 CO-NETIC AA tube purchased from Perfection Mica Corporation [7], 8.0" long and 1 mm thick, The calculated components of the magnetic field strength and intensity are show in Fig. 5 and the total magnetic flux density is shown in Fig. 6. The calculated residual field inside the shield is 0.07 G compared to the measured value of 0.25 G. We note that

this tube had a relatively small length-to-diameter ratio for effective pmt shielding, but long enough that the field in the center of the tube (fairly uniform over the middle 2 inches of the tube) should be representative of a longer tube. This comparison suggests that the calculation underestimates the residual field by a factor of 3.5. These estimates can be compared to the "magnetic shield calculator" from the company which computes the much higher shield effectiveness of 5694 and a residual field of 0.0053 G. This company calculator is consistent with using the maximum value of μ=450,000 for this material. The discrepancy could be due to the actual value of the permeability of the tested shield, but I suspect lower values of μ in parts of the shield are also limiting the measured effectiveness, as suggested by the closer agreement between our calculation and the measurements.

4.2 2" PMT Shields

Many applications require shielding of 2" pmts, and a standard shield is 2.25" in diameter and a thickness of 1 mm. We have calculated the residual field for $H_0 = 50$ (Figs. 7 and 8) for this thickness. The calculated residual fields for 50 G is 0.08 G and an empirical scaling from the previous section suggests a residudal field in side the shield of 0.28 G. For comparison we also plot the residual fields at 50 G and the same outer diameter as before, but with a shield thickness of 0.5 mm. The results are shown in Fig. 9 and Fig. 10. Comparison between this calculation and previous figures shows that this estimate essentially scales with the thickness of the shield as indicated by Eq. 15.

However, for the case of the thin shield of 0.356 mm thickness from Ref. [5] the material begins saturation at 26 G, so we use an effective saturation induction value of half the nominal value (3800 G). This results in a 3.2 G field inside the cylinder. The calculations for this geometry and an external field of $H_0 = 30$ is shown in Figs. 11 and 12.

5 Summary

The magnetic flux and magnetic field intensities have been computed for a cylindrical geometry in a uniform external field perpedicular to the axis of the a long cylinder of magnetic material with permeability μ. The distributions surrounding the magnetic shield have been computed for vaious tube sizes. As long as the material does not saturate, the field inside the cylinder is in the same direction as the external field and reduced in intensity by the standard "effectiveness" factor for cylindrical magnetic shields divided by three.

The effect of saturation of the magnetic material has the consequence that the

shield becomes transparent to the flux in excess of the field where saturation ensues. This field can be computed purely from geometrical factors and the saturation induction of the material. The calculated saturation points are higher than the measured saturation by factors of 1.2 to 2.

In summary, magnetic shield calculations should use values of μ and the saturation induction in the literature scaled down by a factor of about 2.

References

[1] A. Nussbaum. *Electromagnetic Theory for Engineers and Scientists*. Prentice-Hall, Inc., Englewood Cliffs, NJ, 1965. In *Classical Electrodynamics* by J.D. Jackson, the problem is solved for a spherical shell.

[2] Ad-Vance Magnetics. Procurement catalog / engineering manual no.90. Ad-Vance Magnetics, Inc., 625 Monroe St., Rochester, IN, 46975.

[3] Hamamatsu Photonics K.K. *Photomultiplier Tube, Principle to Application: Photon is our Business*, 1994. p. 155.

[4] C.E. Gliniewicz. Magnetic fields surrounding a shield for the photomultiplier tubes in the CLAS TOF. CLAS-NOTE 93-08.

[5] K. Baggett. Chamber versus no chamber measurement comparisons. Magnet Measurement Facility, June 13, 2007. The μ-metal shield is 'amumetal' from Amuneal Manufacturing Corp. http://www.amuneal.com.

[6] J. Flint and E.S. Smith. Tests of phillips XP4312B/D1 pmt in magnetic field. CLAS-NOTE 94-08.

[7] *Magnetic Shield Corporation, Perfection Mica Company*. 740 North Thomas Dr, Bensenville, IL 60106. http://www.magnetic-shield.com.

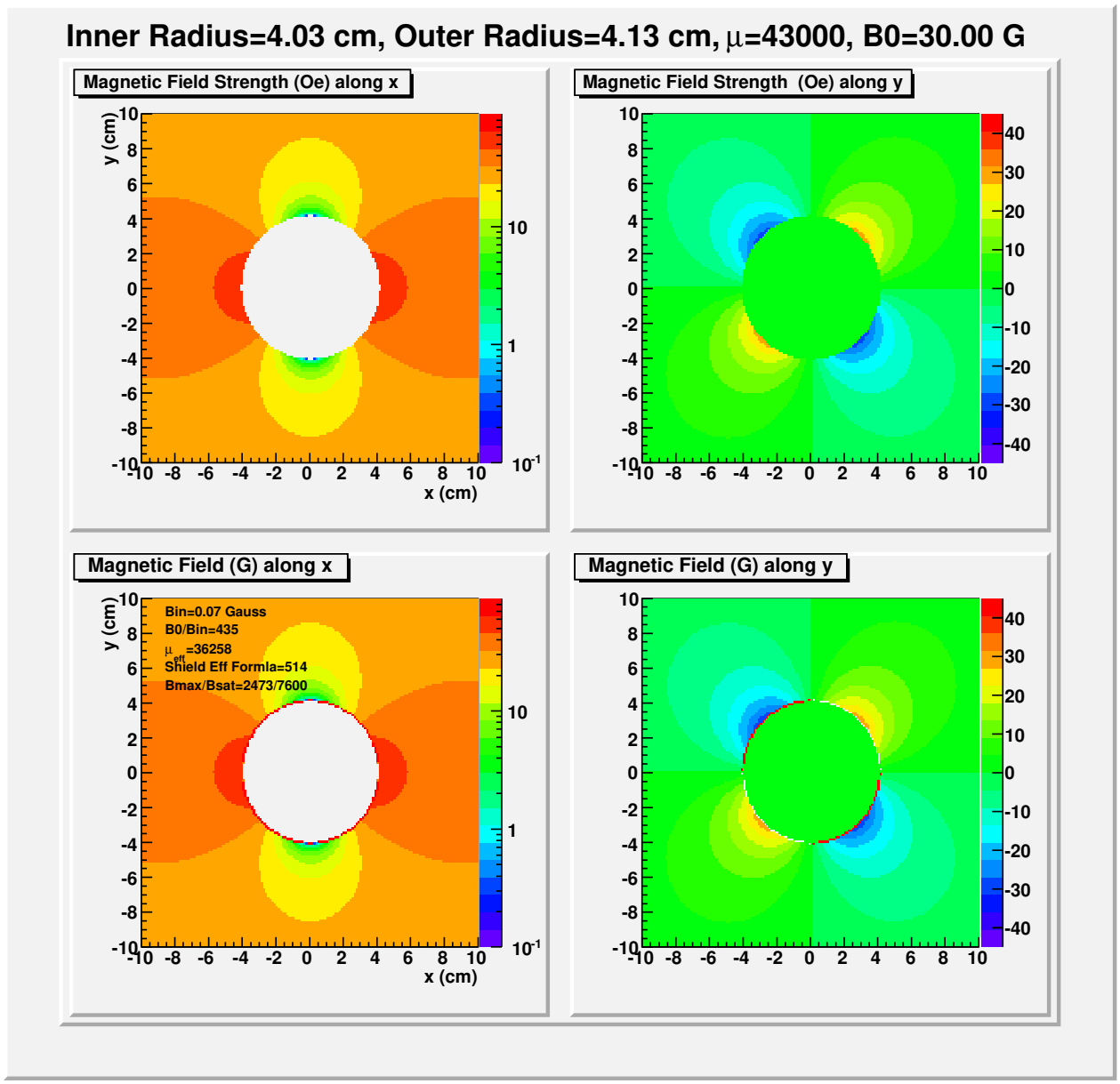

Figure 5: Plots of the magnetic field strength (top) and magnetic flux density (bottom) along the x and y-axis inside a 3.25 in. diameter shield. The unperturbed magnetic field is 30 G in the x-direction.

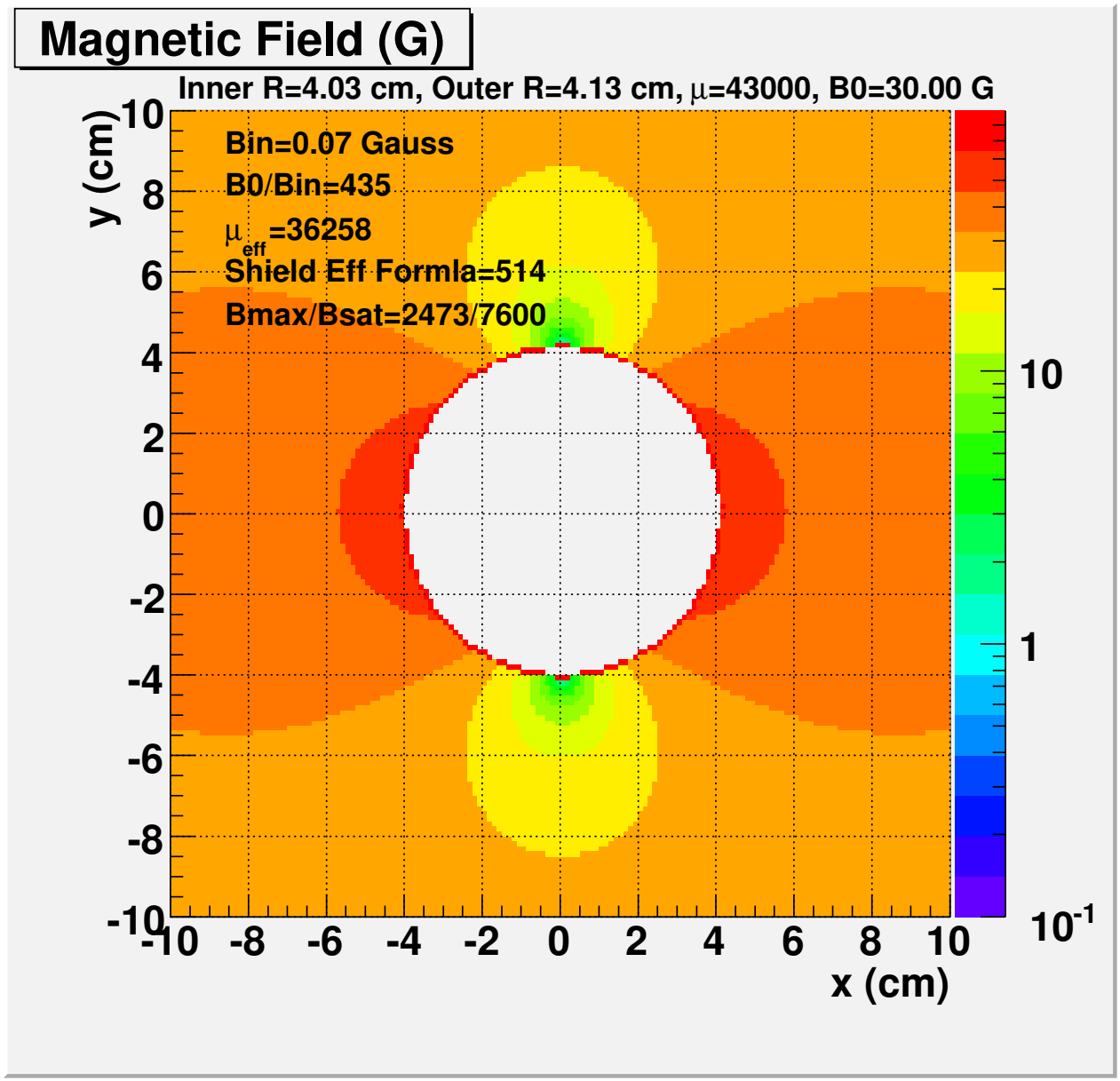

Figure 6: Plots of the total magnetic flux density in a 3.25 in. diameter shield. The unperturbed magnetic field is 30 G in the x-direction. The maximum field in the μ-metal shield is 2473 G below the saturation value of 7600 G. The shield effectiveness is 515 and results in a magnetic field inside the shield of about 0.06 G.This value is to be compared to a measured value of 0.22 G [4].

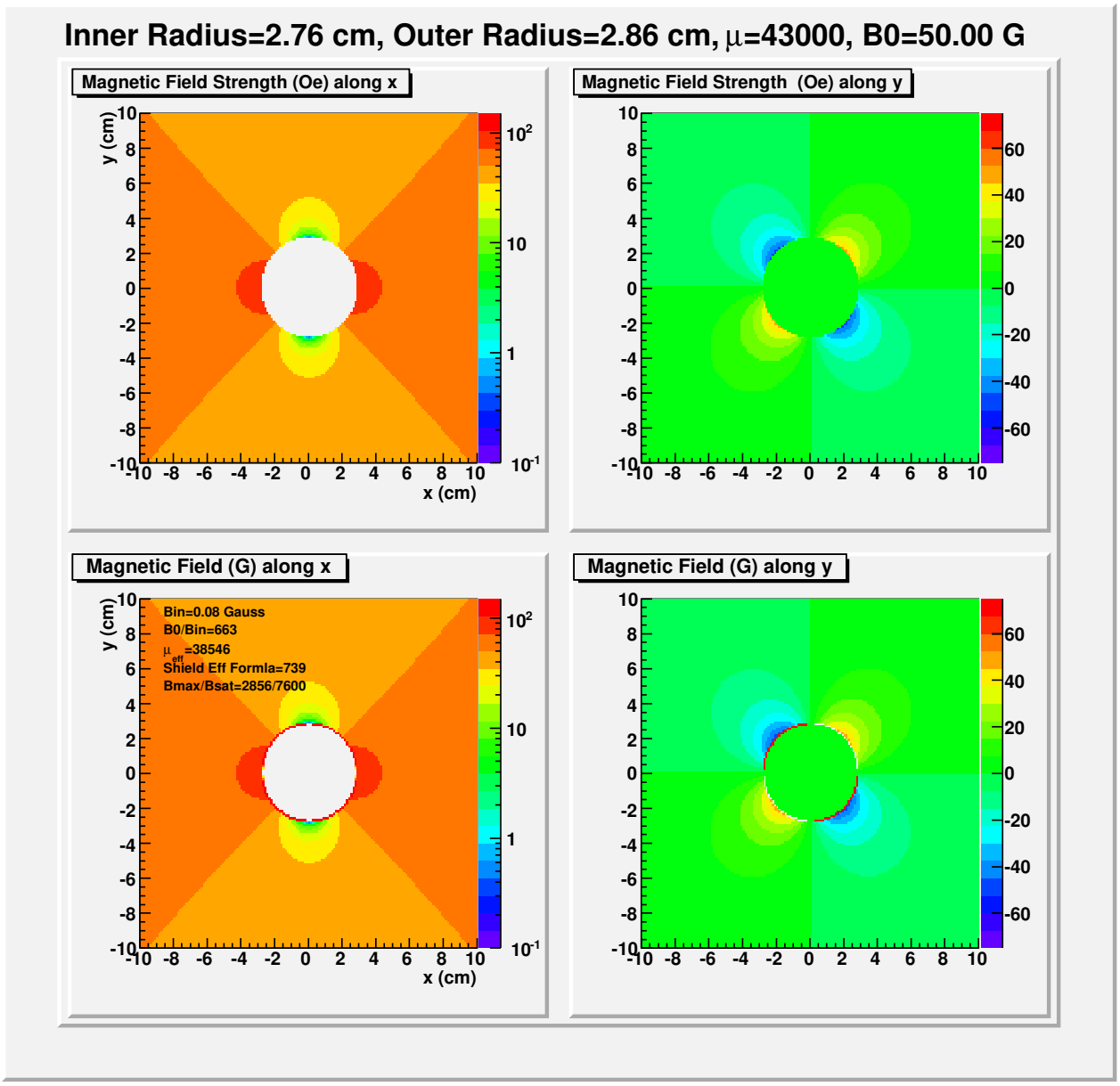

Figure 7: Plots of the magnetic field strength (top) and magnetic flux density (bottom) along the x and y-axis. The unperturbed magnetic field is 50 G in the x-direction.

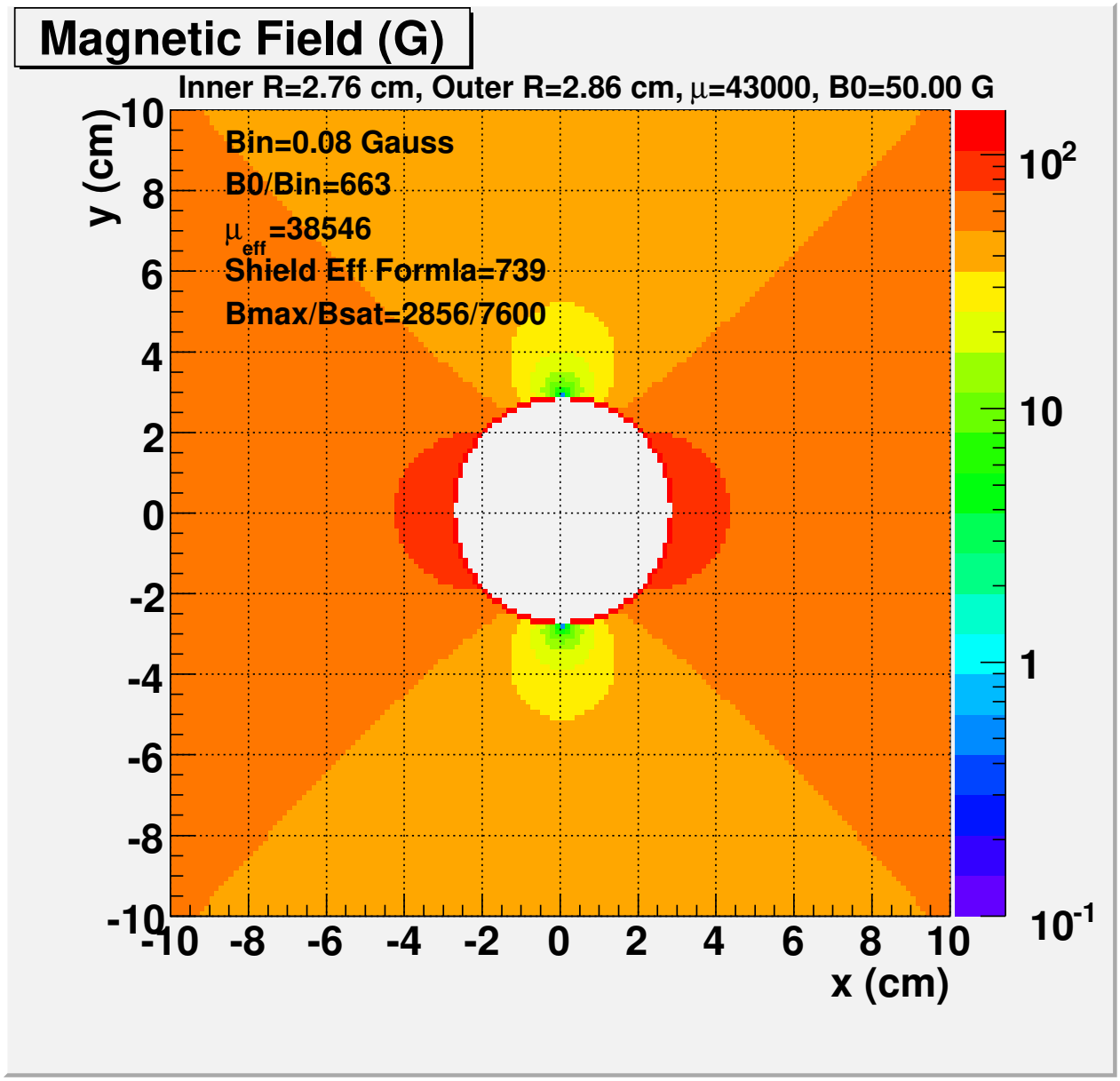

Figure 8: Plots of the total magnetic flux density. The unperturbed magnetic field is 50 G in the x-direction. The maximum field in the μ-metal shield is 2856 G, well below the saturation value of 7600 G. The shield effectiveness is 740 and results in a magnetic field inside the shield of less than 0.1 G.

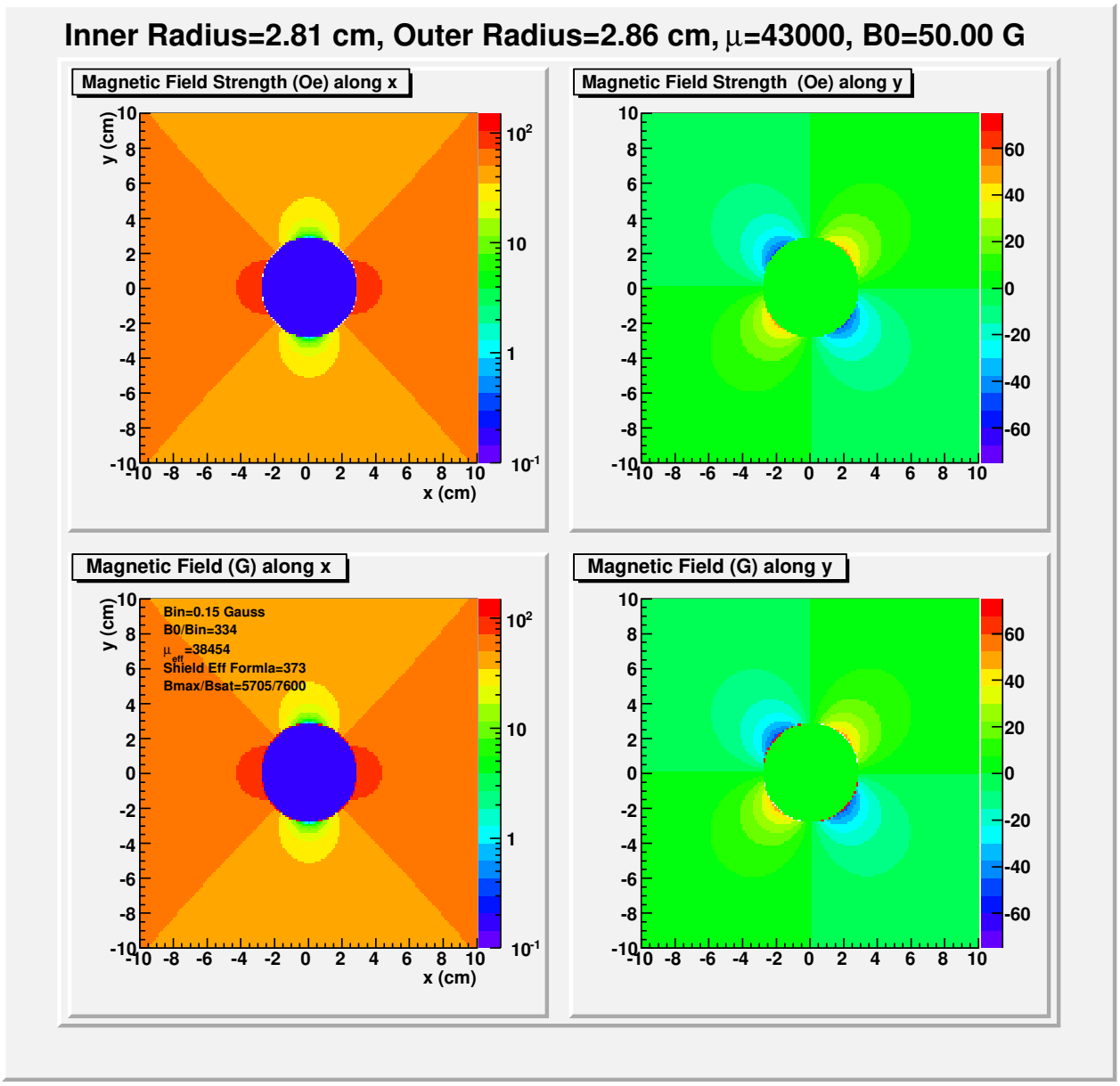

Figure 9: Plots of the magnetic field strength (top) and magnetic flux density (bottom) along the x and y-axis. The unperturbed magnetic field is 50 G in the x-direction.

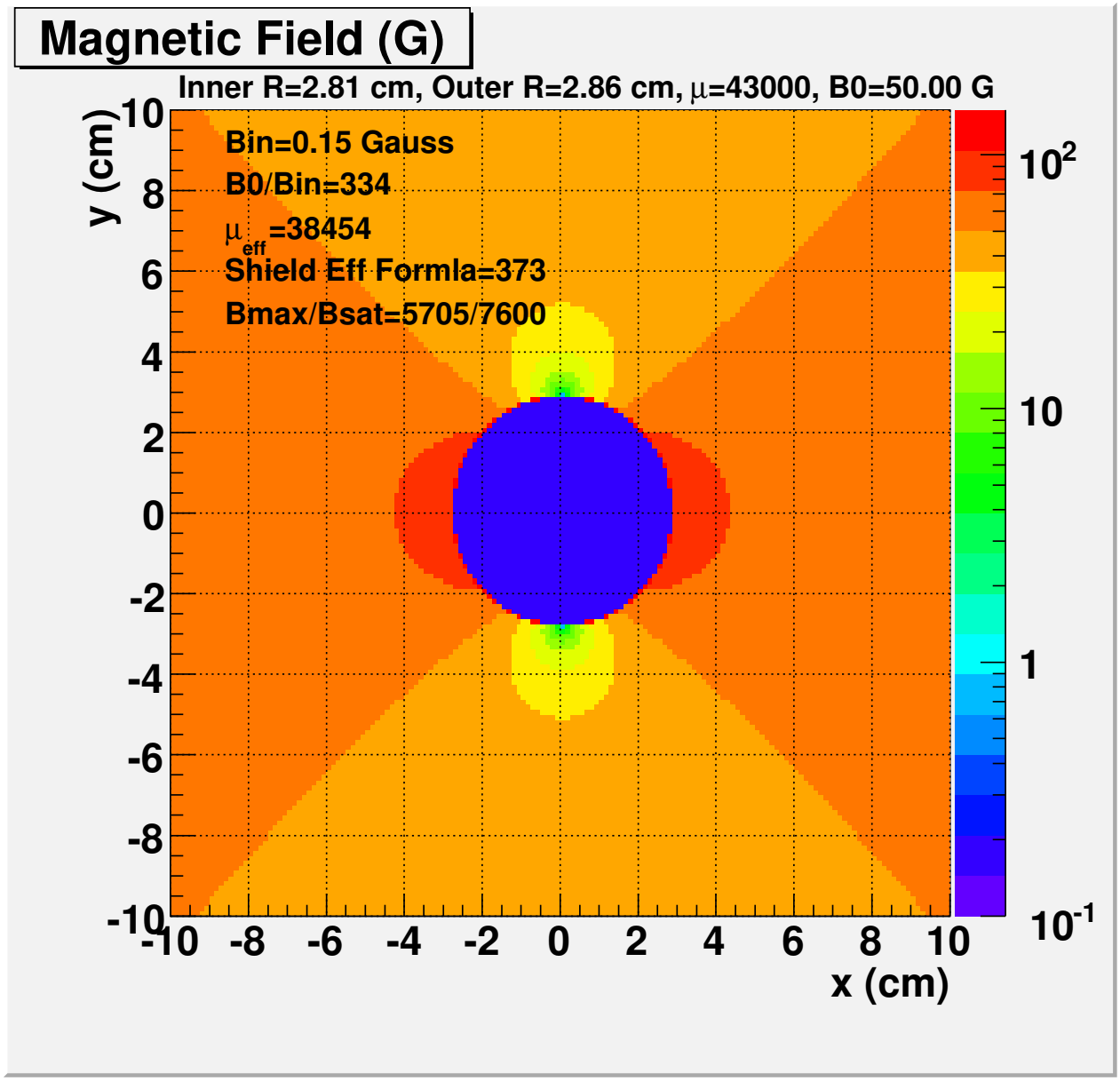

Figure 10: Plots of the total magnetic flux density. The unperturbed magnetic field is 50 G in the x-direction. The maximum field in the μ-metal shield is 5705 G, close to the saturation value of 7600 G. The shield effectiveness is 334 and results in a magnetic field inside the shield of about 0.15 G.

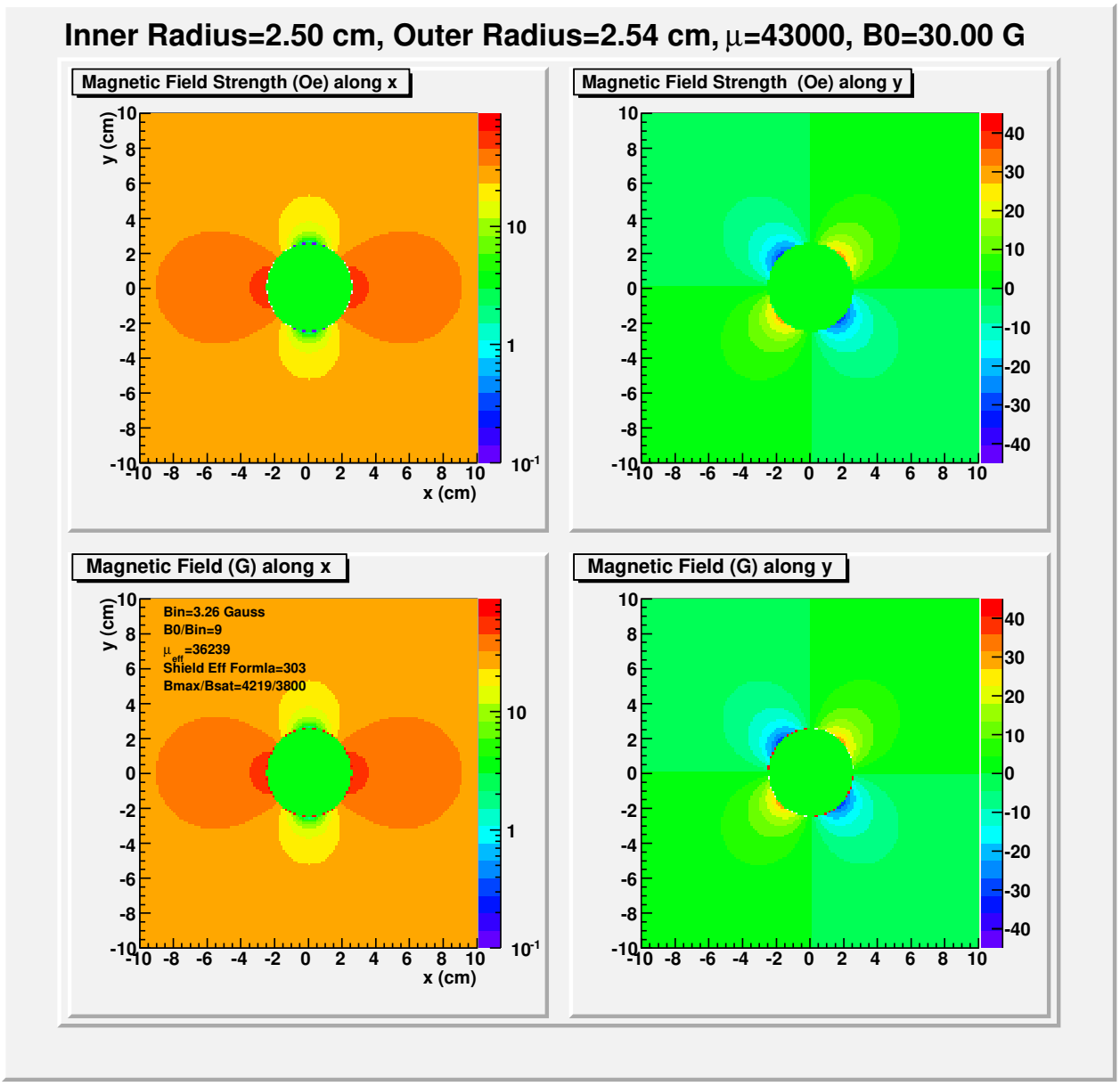

Figure 11: Plots of the magnetic field strength (top) and magnetic flux density (bottom) along the x and y-axis. The unperturbed magnetic field is 30 G in the x-direction. The saturation induction is taken to be half the nominal value.

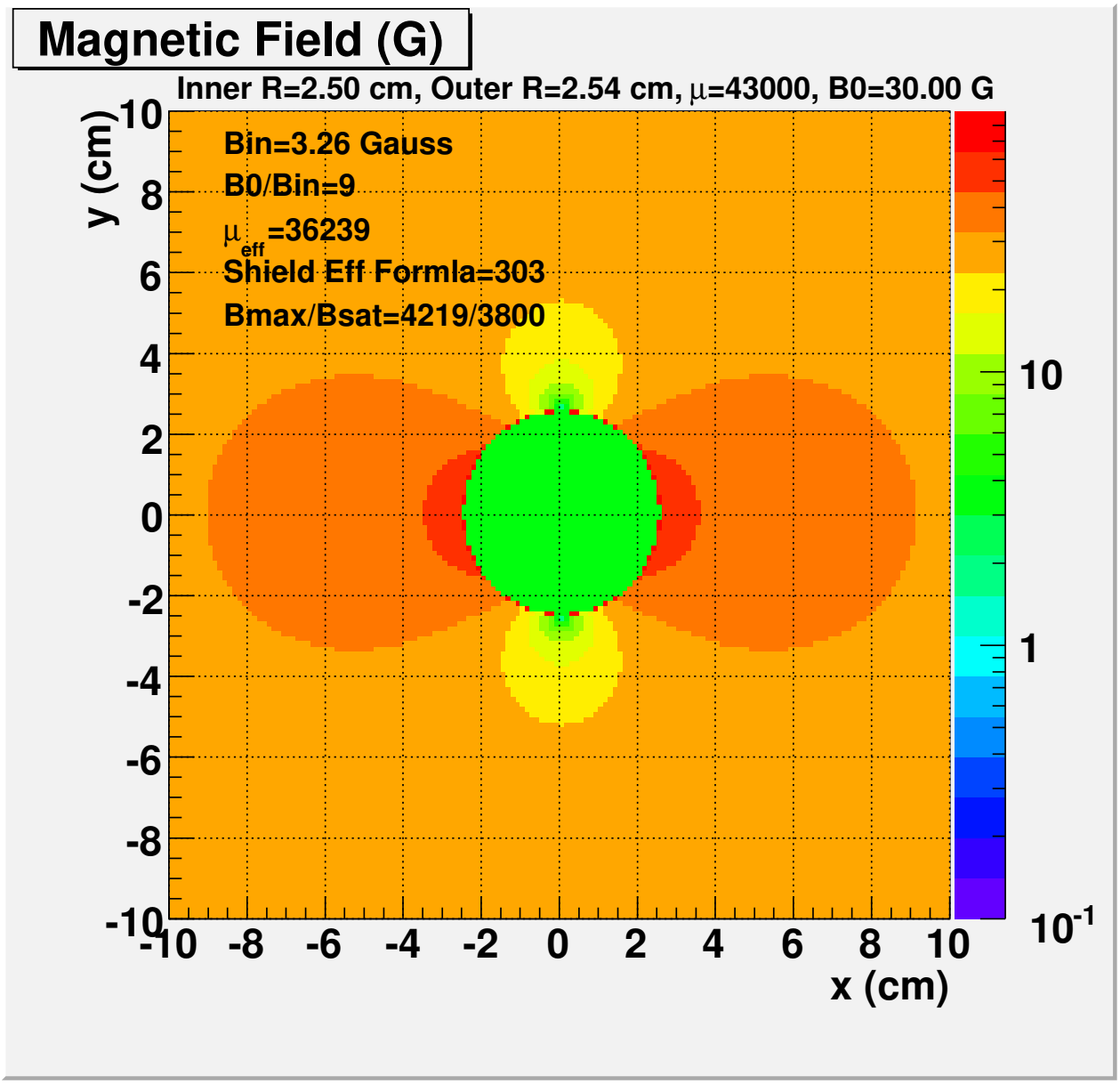

Figure 12: Plots of the total magnetic flux density. The unperturbed magnetic field is 30 G in the x-direction. The maximum field in the μ-metal shield is 4219 G, which exeeds the empirical saturation value of 7600/2 G. The shield thickness is 0.014" with an effectiveness of only 9 because the shield is saturated. This results in a magnetic field inside the shield of about 3.2 G.